Welding in the World (2022) 66:135–144
https://doi.org/10.1007/s40194-021-01186-0

RESEARCH PAPER

# Study on the creep properties of butt fusion–welded joints of HDPE pipes using the nanoindentation test

Shushan Chen[2] · Huan Sheng Lai[1] · Rong Lin[3] · Xie Hang Duan[3]

Received: 31 May 2020 / Accepted: 13 September 2021 / Published online: 14 October 2021


## Abstract

High-density polyethylene (HDPE) pipes have become the preferred water pipes in nuclear power plants. Since the butt fusion–welded joint of HDPE pipes is a weak link of a piping system, it is essential to study the creep properties of the welded joint. In this study, the creep properties of the welded joint of HDPE pipes were studied using a nanoindentation creep test. The test results showed that the weakest creep resistance was not located in the weld center, but was a little away from the weld center. The power-law creep constitutive model was constructed at different locations of the welded joint based on the test results. In addition, the hardness of the welded joint was tested. The results showed that the hardness of the welded joint could reflect the creep resistance of the welded joint.

**Keywords** HDPE · Creep · Nanoindentation · Welded joint · Butt fusion weld

**Nomenclature**

| | |
|---|---|
| $A$ | Projected contact area |
| $c$ | Constant depending upon the geometry of the indenter |
| $F$ | Applied load |
| $H$ | Hardness |
| $h$ | Contact depth |
| $h_{pc}$ | Creep displacement |
| $n$ | Power-law creep stress exponent |
| $\dot{\varepsilon}$ | Creep strain rate |
| $\sigma$ | Stress |
| $\lambda$ | Power-law creep constant |

Recommended for publication by Commission XI - Pressure Vessels, Boilers, and Pipelines

✉ Huan Sheng Lai
sheng158@hotmail.com

1 Sino-French Institute of Nuclear Engineering and Technology, Sun Yat-sen University, Zhuhai 519082, China

2 China Nuclear Power Design Co., Ltd., Shenzhen 518031, China

3 School of Chemical Engineering, Fuzhou University, Fuzhou 350116, China

## 1 Introduction

Pipeline is one of the main means to transport oil, water, and natural gas, which plays a crucial role in the development and stability of the national economy. Compared with the traditional metal pipes, high-density polyethylene (HDPE) pipes have the advantages of corrosion resistance, good flexibility, and long service life. Therefore, HDPE pipes have become the first choice for water pipes in nuclear power plants [1].

Due to manufacturing technology, the length of HDPE pipes with large size (larger than 90 mm) was usually less than 10 m. They need to be welded together to create a good airproof and well-structured piping system in order to satisfy the engineering applications, such as water delivery. Butt fusion welding is one of the simplest and most effective welding methods for polyethylene pipes [2]. The method of butt fusion welding is to locally melt two pipe ends with a heating plate. After fully absorbing heat, pipes are contacted together with a proper axial compression force, and then welding is completed after pressure holding and temperature cooling. However, in a pipeline system, the pipe welded joint usually becomes the weak link since the welding causes the degradation of material properties and defects (notches, cracks, cavities, etc.) possibly existing in the joint [3]. Since the HDPE pipeline began to be used in the water supply system of Catawba nuclear power plant in 1998, the structural integrity and service life of butt fusion joints of the HDPE pipeline have been highly concerned by the U.S. Nuclear Regulatory Commission (USNRC) [4]. Therefore, a study of butt fusion–welded joints of HDPE pipes is of great significance to ensure the structural integrity of HDPE pipes.

Tensile tests and burst tests can be used to evaluate the short-term mechanical properties of HDPE pipe welded joints [5]. However, the HDPE piping system in nuclear power plant is required to service more than 60 years, so it should study the long-term performance of HDPE pipe welded joints, because HDPE pipe creeps significantly even at room temperature and under low load level [6]. Troughton et al. [7, 8] have found that the traditional creep test is more effective than the hydrostatic test in evaluating the welded joints on the long-term performance. However, the traditional creep test usually takes a long time and it is difficult to obtain the creep properties of the welded joints by the test.

Nanoindentation testing, being a relatively fast and nondestructive method, has been employed widely and accepted as one of the useful methods for determining the mechanical properties of many materials [9]. Because of the short test cycle, simple specimen preparation, high test accuracy, and applicability to micro-volume materials, it has been increasingly employed for plastics characterization recently [10]. Oliveira et al. [11] studied the effect of aging on the nonlinear tensile creep of HDPE and the creep behavior was predicted. Lach et al. [12] summarized the application of microindentation technology in different polymer welded joints and found out the different change rules of elastic modulus of different materials on the melting line. Shaheer et al. [13] found that the butt fusion–welded joint had a melt zone, where the material was melted during the welding operation, and also had a heat-affected zone. Huang et al. [14] investigated the nanoindentation creep of three polymeric materials to measure the nanoindentation creep stress exponents. However, the creep behavior of HDPE pipe welded joints is still unknown.

In this paper, the creep behavior of HDPE pipe welded joints was researched using the nanoindentation test. Tests were conducted at room air temperature (25 °C). Then, creep constitutive models were obtained at different locations of the welded joints based on the test results. In addition, the hardness of welded joints was tested.

## 2 Experimental

### 2.1 Materials and specimens

HDPE PE100 pipes were used with an outside diameter of 200 mm and a wall thickness of 18.2 mm. The standard dimension ratio (SDR) was hence 11. The pipes were welded according to the standard ISO 21307 using a butt fusion welding machine with the model HDC160-315, which was produced by Huida Pipeline Technology Co., Ltd., China. According to ISO 21307, welding parameters are formulated as shown in Table 1.

The welded joint can be roughly divided into three parts, which are melt zone (MZ), heat affected zone (HAZ), and parent material (PM) [13], as shown in Fig. 1. The creep properties of each part are different. Therefore, four specimens were machined out from the welded joints every 3 mm away from the weld centerline, and they were numbered as $0^{\#}$, $3^{\#}$, $6^{\#}$, and $9^{\#}$ which represented 0, 3, 6, and 9 mm away from the weld centerline for each specimen respectively, in which $0^{\#}$ was sized 5 × 18.2 × 15 mm, $3^{\#}$ was sized 5 × 18.2 × 12 mm, $6^{\#}$ was sized 5 × 18.2 × 9 mm, and $9^{\#}$ was sized 5×18.2 × 6 mm, and the surface center area was tested for each specimen, as shown in Fig. 2. For comparison, a specimen sized 10 × 10 × 10 mm was prepared from PM. The test surfaces were polished with high precision using the Leica EM TXP machine.

### 2.2 Nanoindentation testing

Nanoindentation tester NHT$^2$ from Anton Parr with pneumatic isolation system, top surface referencing ring, and cabinet enclosure was used to carry out the test. The top surface referencing ring significantly decreases the frame compliance and the frame length, and brings about extremely low frame compliance (0.1 nm/mN) and thermal drift (0.015 nm/s). Therefore, the thermal drift effect of the system is automatically deducted, so that the effect of thermal drift on the measurement results is minimized [15]. Three-sided diamond pyramid Berkovich indenter was used. Tests were performed at room air temperature, i.e., 25 °C. Nanoindentation was done in a load-controlled manner. First, the load was increased to an expected value which was marked as applied load with a loading rate of 150 mN/min. And then the load was held constant for a period of 1200 s. Finally, the load was decreased to 0 mN with the same rate of 150 mN/min. The applied load is shown in Table 2 for all specimens. As shown in Table 2, seven different applied loads were tested for the PM specimen, but only one fixed applied load was tested for specimens in the

**Table 1** Parameters of butt fusion welding

| Item | Value |
|---|---|
| Heater plate temperature (°C) | 210 |
| Bead-up pressure (MPa) | 0.15 |
| Bead-up size (mm) | 2 |
| Heat soak time (s) | 182 |
| Heat soak pressure (MPa) | 0.02 |
| Heater plate removal time (s) | 5 |
| Fusion jointing time (s) | 8 |
| Cooling time (min) | 23 |

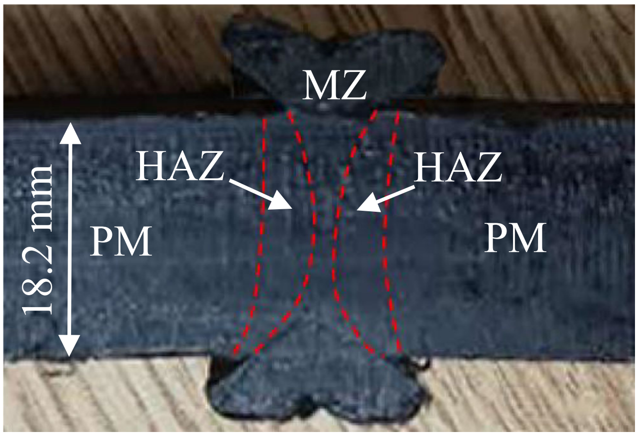


**Fig. 1** A typical butt fusion–welded HDPE pipe joint with an outside diameter of 200 mm and a wall thickness of 18.2 mm

joint. The reason would be explained in the following section. The load and displacement were recorded automatically during the test. The creep data were acquired from the normal force versus penetration depth curves generated by a computer [16]. Only the holding process was used for analysis. Three tests were performed independently on the specimen surface under each applied load. Each indentation position was separated by at least 0.5 mm in order to ensure that the test result was not affected by each other. Each test position was arranged around the surface center of the specimen as shown in Fig. 2, where the small white triangles represented the indentation positions.

The typical indentation on the specimen surface just after the indentation test is shown in Fig. 3. It could be seen that the specimen surface left an irrecoverable indentation similar to that of the indenter, and the material in the contact area of the indenter was squeezed, which was caused by creep deformation and possibly with plastic deformation. Note that all specimens had a similar indentation on the specimen surface after the indentation test.

# 3 Results and discussion

## 3.1 HDPE creep behavior

A creep curve usually can be divided into three distinct phases: primary stage, steady-state stage, and tertiary stage [17]. However, the nanoindentation creep curve only consists of two stages, which are primary and steady-state creep states as shown in Fig. 4 [14]. The slope of the steady-state curve is nearly constant and represents the mean creep rate [17].

The formulation of steady-state creep is basically followed according to the concept of Goodall and Clyne. The steady-state strain rate of conventional tensile creep satisfies the power law [18]:

$$\dot{\varepsilon} = \lambda \sigma^n \tag{1}$$

where $\dot{\varepsilon}$ is the creep strain rate, $\sigma$ is the applied stress, $\lambda$ is the power-law creep constant, and $n$ is the power-law creep stress exponent. $\sigma$ is calculated by:

$$\sigma = F/A \tag{2}$$

where $F$ is the applied load and $A$ is the projected contact area. For the used Berkovich indenter in this paper, $A = 24.56h_{pc}^2$, where $h_{pc}$ is the creep displacement. The calculation of hardness in the nanoindentation technique is identical to that of $\sigma$, which is calculated by Lucas et al. [19]:

$$H = \sigma = \frac{F}{A} = \frac{F}{ch^2} \tag{3}$$

where $H$ is the hardness, $h$ is the contact depth, and $c$ is a constant depending on the geometry of the indenter ($c$ = 24.56 for the Berkovich indenter in this paper).

$\dot{\varepsilon}$ during the indentation period is defined as Mayo and Nix [20]:

$$\dot{\varepsilon} = \frac{1}{h}\frac{dh_{pc}}{dt} \tag{4}$$

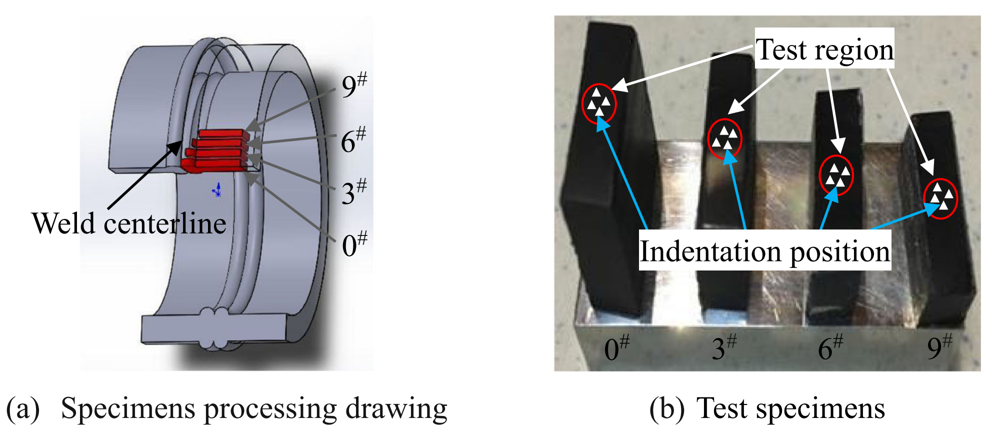


**Fig. 2** Nanoindentation test specimens. **a** Specimens processing drawing. **b** Test specimens

**Table 2** Loading conditions for all specimens

| Item | Value |
|---|---|
| Loading rate (mN/min) | 150 |
| Unloading rate (mN/min) | 150 |
| Holding time (s) | 1200 |
| Applied Load (mN) | 25 mN for the specimen of $0^{\#}$, $3^{\#}$, $6^{\#}$, and $9^{\#}$ |
| | 10, 15, 20, 25, 30, 35, and 40 mN for PM specimen |

Therefore, the stress exponent $n$ is calculated by:

$$n = \frac{\partial \ln \dot{\varepsilon}}{\partial \ln \sigma} = \frac{\partial \ln\left(\frac{1}{h_{pc}} \frac{dh_{pc}}{dt}\right)}{\partial \ln\left(\frac{F}{24.56 h_{pc}^2}\right)} \quad (5)$$

## 3.2 Parent material

The test results are shown in Fig. 5. Note that three curves were obtained at each applied load because three tests were performed at each applied load, but only one curve at each applied load is shown in Fig. 5 because they were similar. In the following figures, also only one curve at each applied load was shown in the figure. It could be found that the indentation displacement increased with the increase of load. The variations of creep displacement with creep time at different loads are shown in Fig. 6. As shown in Fig. 6, the creep displacement increased with the increase of the applied load. The main reason was that the larger the load was, the larger the creep deformation would be. When the creep time increased to about 300 s, the slope of the curves under different applied loads was stable. After this time, the slope hence was independent of the applied load, while dependent on the material properties.

According to the experimental data in Fig. 6, the stress and creep strain rate under a constant load could be calculated using the equations in Section 3.1. In order to improve the accuracy, the curve of indentation creep deformation showing a stable state should be selected for calculation. The curve of $\ln \dot{\varepsilon} \ln \sigma$ is drawn as shown in Fig. 7, whose slope was the value of exponent $n$ for HDPE.

As shown in Fig. 7, the curves almost had an identical slope. It meant that the effect of load on $n$ was small. The values of $n$ and $\lambda$ were obtained from the curves under different loads and are listed in Table 3, where the values at each applied load were average values of three tests because three tests were performed at each applied load. In the following tables, the values of $n$ and $\lambda$ were also average values. The average values of $n = 15.65$ and $\lambda = 8.64\text{E}{-27}\ \text{GPa}^{-n}$/s be the creep properties for the parent material of HDPE. Thus, a power-law creep constitutive model was obtained for the parent material of HDPE:

$$\dot{\varepsilon} = 8.64\text{E} - 27\sigma^{15.65} \quad (6)$$

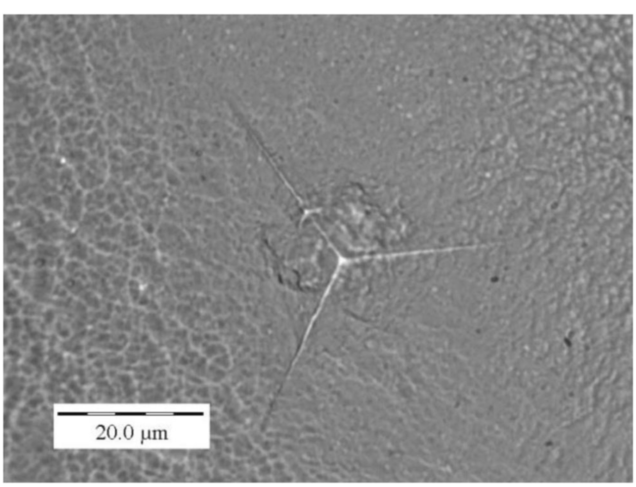


**Fig. 3** Typical indentation on the specimen surface just after the indentation test

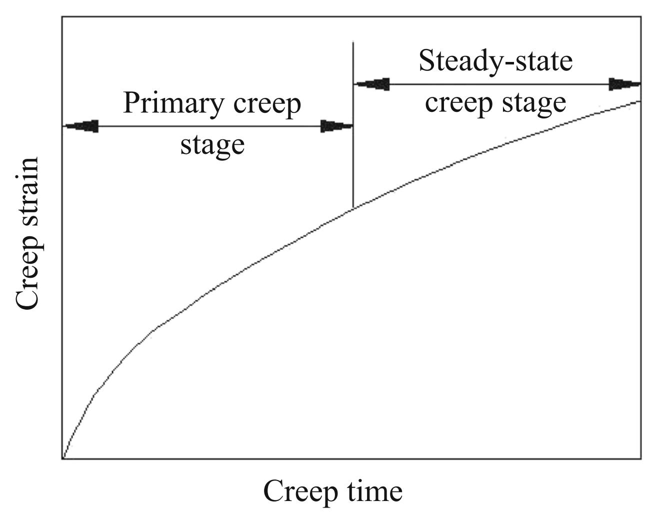


**Fig. 4** Typical indentation creep curve [14]

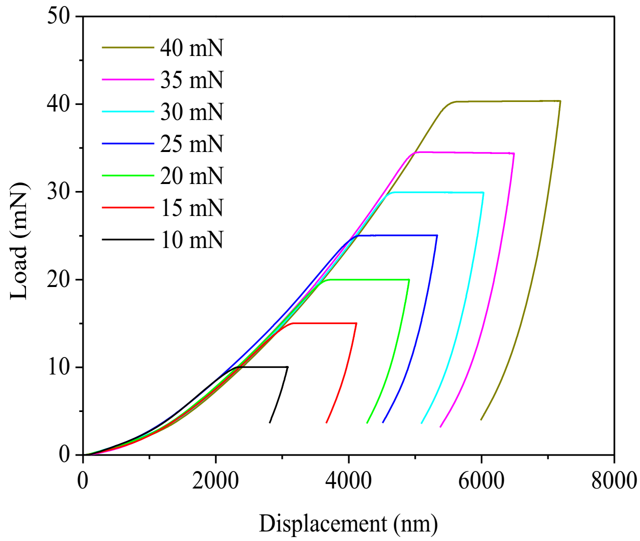


**Fig. 5** Relationship between the indentation load and the displacement in PM

### 3.3 Welded joint

As shown in Table 3, $n$ and $\lambda$ were affected by the applied load and their average values were close to the values at the applied load of 25 mN. Therefore, a fixed load of 25 mN was used in the nanoindentation creep test for the four welded specimens in order to compare the creep displacement curves at different locations of the joint, because the creep displacement curves are affected by the applied load as shown in Fig. 6.

The comparisons of load-displacement curves between welded and parent material specimens are shown in Fig. 8, which showed different changing trends. This was caused by the variations of material properties, such as creep properties and elastic properties (Fig. 9a [21, 22]), at the welded joint.

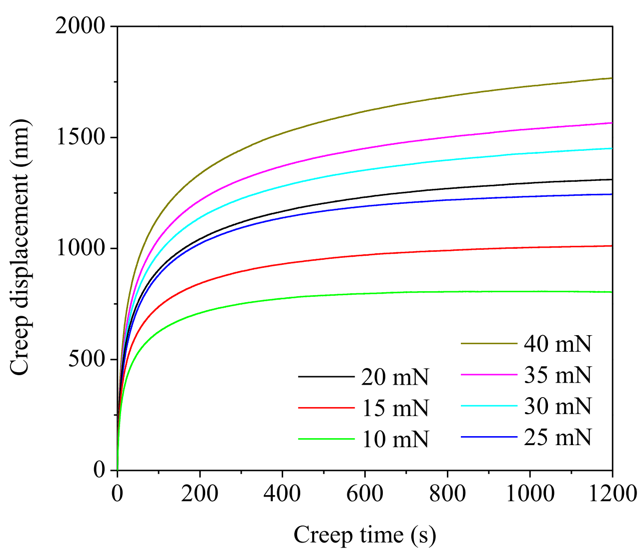


**Fig. 6** Change of the creep displacement in PM with time under different loads

The polarized light with visible changes in the butt fusion welding joint is shown in Fig. 9b [21, 22]. As shown in Fig. 9b, the center of the welded joint had the highest degree of crystallinity (marked by the red color) and the non-heated regions had the lowest. The reason was that in the heating stage of the butt fusion welding, the pipe ends were heated by a heating plate with the temperature of 210 °C, and the scope of the melting zone gradually expanded with increase of the heat soak time, as shown in Fig. 10a. Note that the heat soak time was 128 s and the melting point was about 130 °C for HDPE. Due to the effect of axial extrusion pressure of 0.02 MPa, the molten HDPE flowed along the radial direction as a whole. In the cooling stage, the molten HDPE continued to flow along the radial direction due to the application of axial extrusion pressure of 0.15 MPa, as shown in Fig. 10b. With the decrease of temperature, the original molecular chain orientation would be retained around the boundary of the melting region and the unmelted region due to the existence of velocity gradient [23].

Figure 11 shows the comparisons of creep displacement-time curves between welded and parent material specimens under the same applied load of 25 mN. At the end of the creep time, i.e., 1200 s, the larger the creep displacement (i.e., the higher the ordinate value in Fig. 10) was, the weaker the creep resistance was, because they all suffered identical applied load and creep time. Therefore, as shown in Fig. 11, specimen 3# had the largest creep displacement, which means that the creep resistance at the location of 3 mm away from the welding center was the weakest. The creep resistance at the location of 9 mm away from the welding center was larger than that at the welding center, but smaller than that of the parent material. The creep resistance was the strongest at 6 mm from the welding center.

In order to construct the creep constitutive equation of the welded joint, the same calculation was done as that of the parent material specimen in Section 3.2. As shown in Fig. 12, there were differences in the slopes of $\ln \dot{\varepsilon} - \ln \sigma$ curves for welded specimens. The results are shown in Table 4. It was found that specimen 6# had the largest value of $n$ (20.75), while the smallest value of $n$ (14.98) appeared in specimen 3#. For the value of $\lambda$, specimen 3# had the maximum value (3.49E−26 GPa$^{-n}$/s), while the smallest value (4.37E−35 GPa$^{-n}$/s) appeared in specimen 9#.

### 3.4 Hardness test

Hardness testing is widely used to study the mechanical properties of metals and ceramics due to a direct correlation between hardness and yield strength of these materials. As a relatively simple and rapid testing technology, microhardness testing has been widely used and is considered to be one of the

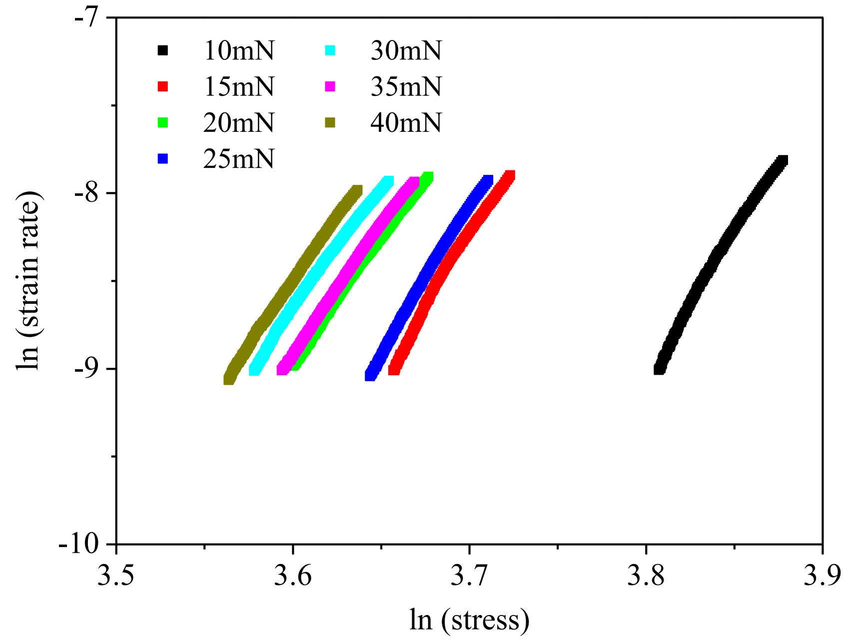


**Fig. 7** $\ln\dot{\varepsilon}\ln\sigma$ curves of the parent material of HDPE at different loads

effective methods to measure the mechanical properties of various materials [10]. In this paper, Vickers hardness was tested for the HDPE pipe welded joint. The hardness for all five specimens in the nanoindentation creep test was tested in the same region. A load of 0.1 kgf was applied and held for 10 s. Three tests were performed for each specimen, and the values were then averaged, as shown in Table 5.

The comparison of $n$ and the hardness of welded and parent material specimens are shown in Fig. 13. As shown in Fig. 13, the variation of $n$ and the hardness had the same trend. The maximum hardness appeared in the welded joint. Lach et al. [12] found that for semicrystalline polymers (HDPE), the maximum hardness and indentation modulus mostly appeared in the welded joint. Zeng et al. [24] showed that the hardness of HDPE would be greatly increased after heating and connected under axial pressure. The variation of $\lambda$ with the hardness is shown in Fig. 14. As shown in Fig. 14, it was difficult to find the relationship between $\lambda$ and hardness. The creep resistance was dependent on the two parameters of $n$ and $\lambda$. Therefore, it was not easy to find the relationship between hardness and creep resistance for HDPE according to Figs. 13 and 14.

However, for the butt fusion–welded joint, it was found that the smallest hardness appeared in specimen 3 #, the largest hardness located in specimen 6 #, and specimens 0 # and 9 # almost had identical hardness, as shown in Fig. 13. This phenomenon was in accordance with the variation of the creep displacement as shown in Fig. 11. Note that the weakest creep resistance appeared in specimen 3 # and the creep resistance of specimen 3 # was weaker than the parent material, as shown in Fig. 11. This phenomenon was different from the variation of hardness as shown in Fig. 13, where specimen 3 # had slightly larger hardness than the parent material, as shown in Fig. 13. This was possibly induced by the test error as shown in Table 5, where the standard deviation (0.13) of specimen 3 # was larger than the parent material (0.08). Therefore, a concluded could be obtained that the lower the hardness, the weaker the creep resistance for a butt fusion welding joint. In fact, similar results have been found by other researchers [25, 26] and the hardness has been used to predict the creep life [26, 27].

**Table 3** Creep parameters at different loads

| Parameter | Load (mN) | | | | | | | Average value |
|---|---|---|---|---|---|---|---|---|
| | 10 | 15 | 20 | 25 | 30 | 35 | 40 | |
| $n$ | 17.14 | 16.86 | 15.47 | 16.26 | 14.57 | 14.64 | 14.61 | 15.65 |
| $\lambda$ ($GPa^{-n}$/s) | 5.90E−33 | 3.32E−31 | 2.24E−27 | 1.46E−29 | 1.75E−26 | 2.27E−26 | 1.79E−26 | 8.64E−27 |

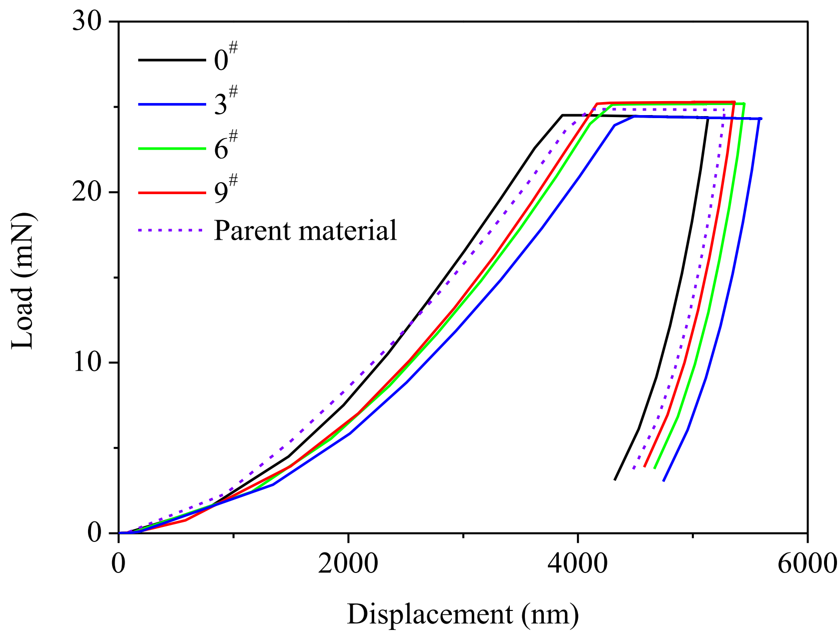


**Fig. 8** Comparison of load-displacement curves between welded and parent material specimens

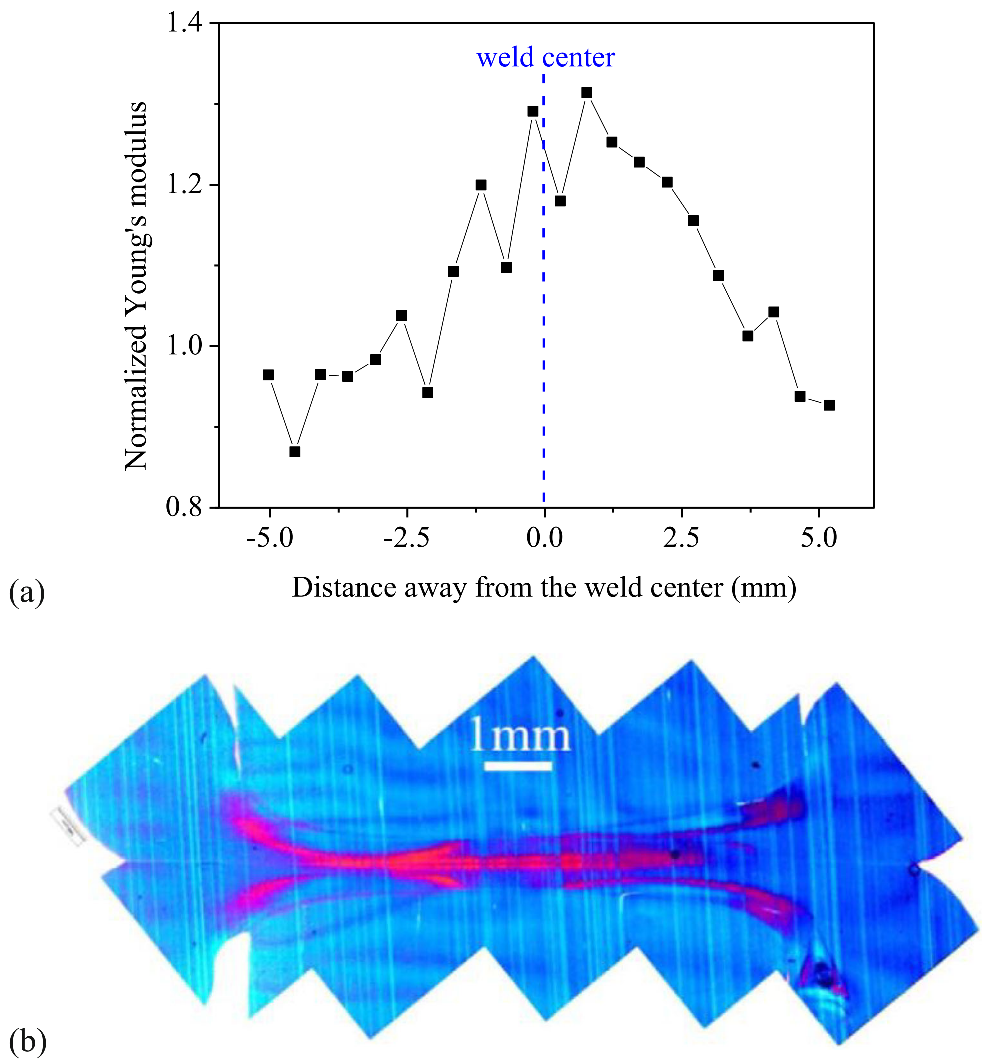


**Fig. 9** **a** Normalized Young's modulus of the HDPE butt fusion welding joint [21, 22] and **b** optical micrograph of the HDPE butt fusion welding joint in polarized light [21, 22]

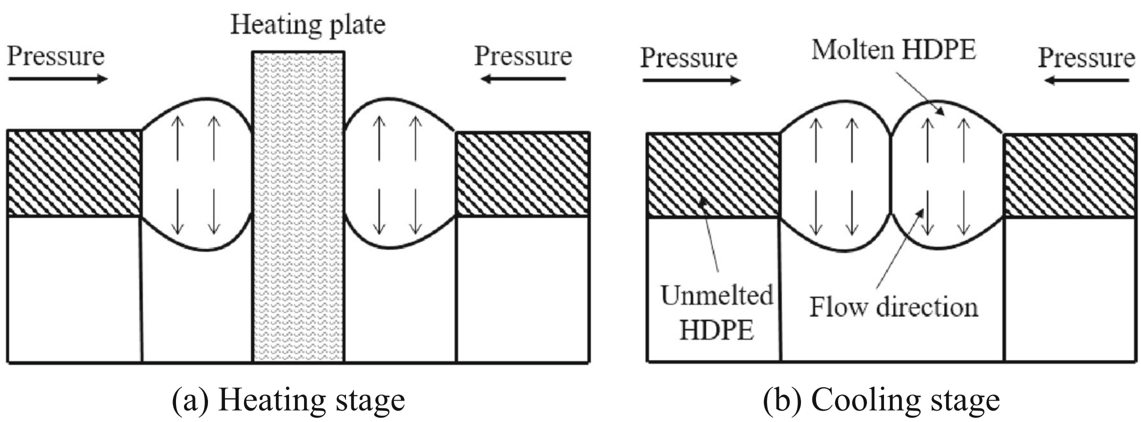


**Fig. 10** Flow direction of molten HDPE during the butt fusion welding [23]. **a** Heating stage. **b** Cooling stage

**Fig. 11** Comparison of displacement-time curves among welded and parent material specimens at the load of 25 mN

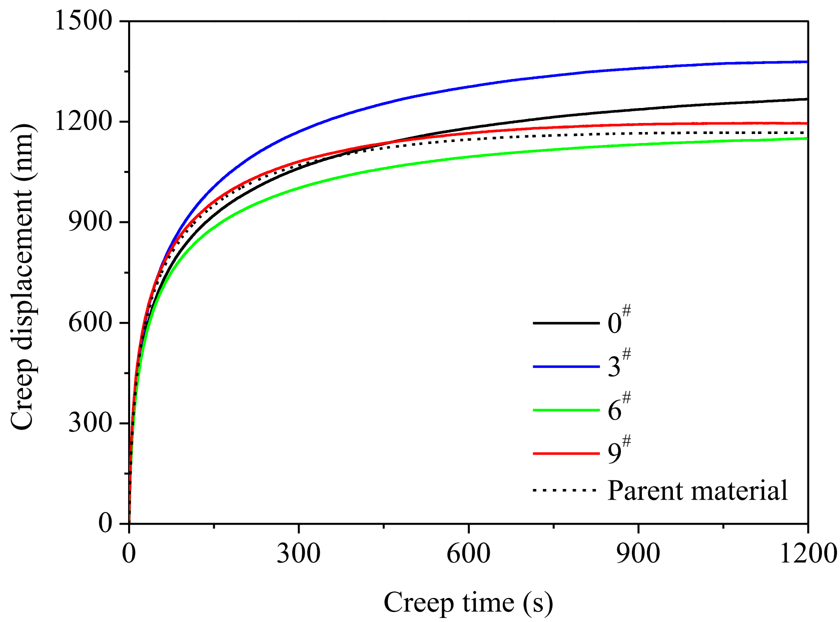


**Fig. 12** $\ln\dot{\varepsilon} - \ln\sigma$ curves of welded specimens at 25 mN

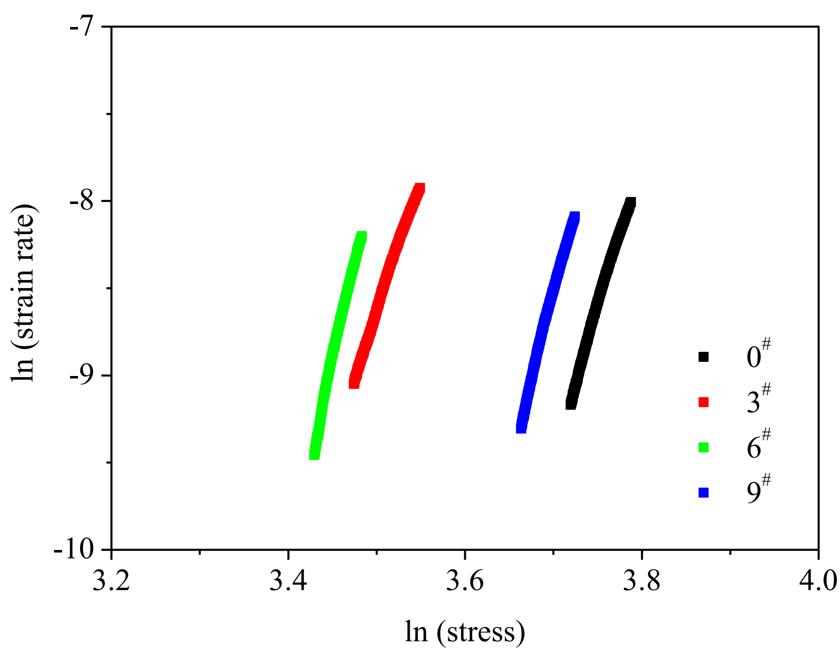

**Table 4** Creep parameters of welded specimens

| Specimen | 0# | 3# | 6# | 9# |
|---|---|---|---|---|
| $n$ | 19.21 | 14.98 | 20.75 | 19.62 |
| $\lambda$ (GPa$^{-n}$/s) | 7.58E−31 | 3.49E−26 | 2.26E−34 | 4.37E−35 |

**Table 5** Vickers hardness of welded and parent material specimens

| Specimen | 0# | 3# | 6# | 9# | Parent material |
|---|---|---|---|---|---|
| Hardness (HV) | 4.98 | 4.63 | 5.12 | 4.77 | 4.47 |
| Standard deviation | 0.23 | 0.13 | 0.08 | 0.08 | 0.08 |

## 4 Conclusions

In this paper, the creep properties of HDPE pipe welded joints were carried out using nanoindentation creep test. The hardness of the welded joints was also tested. The following main conclusions were reached:

(1) The nanoindentation creep test results showed that the weakest creep resistance was located 3 mm away from the welding center and the strongest creep resistance was located 6 mm away from the welding center. Therefore, creep failure usually occurred in welded joints for the long-term service of HDPE pipes.

(2) Based on the nanoindentation creep test results, the power-law creep constitutive model of HDPE was

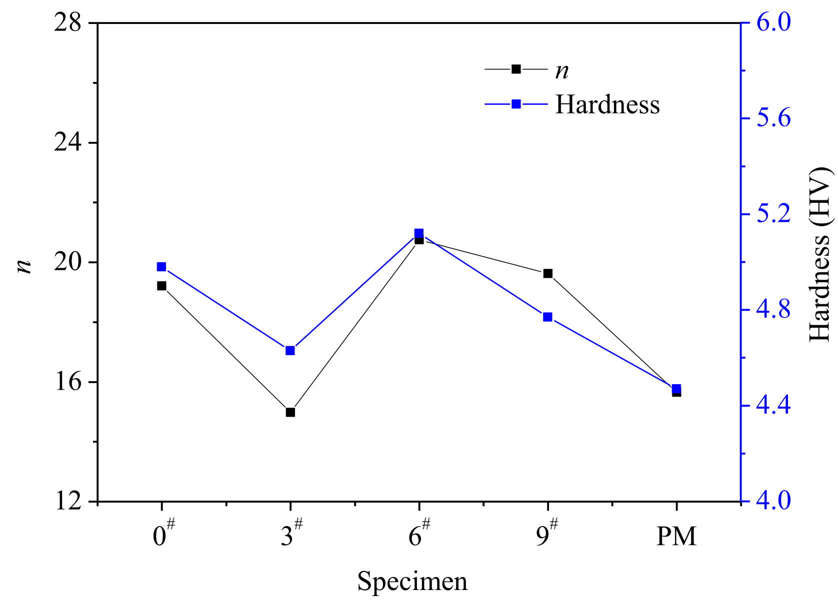


**Fig. 13** Comparison of $n$ and hardness for welded and parent material specimens

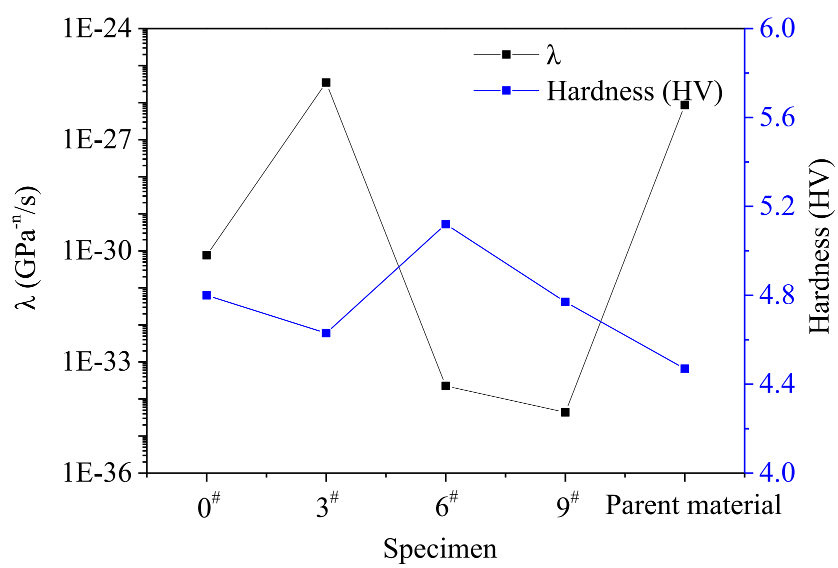


**Fig. 14** Comparison of $\lambda$ and hardness for welded and parent material specimens

obtained at different locations of the welded joint. The power-law creep stress exponent ranged from 14.98 to 20.75 and the power-law creep constant ranged from 4.37E−35 to 3.49E−26 $GPa^{-n}$/s in the welded joint. The variations of power-law creep constant and stress exponent were due to the butt fusion welding changing the creep properties of the joint.

(3) The hardness test results showed that the smallest hardness of the welded joint located 3 mm away from the welding center corresponding to the weakest creep resistance of the joint, and the largest hardness of the welded joint located 6 mm away from the welding center corresponding to the strongest creep resistance of the joint. Therefore, the hardness of the welded joint could reflect the creep resistance.

**Acknowledgements** This work was supported by the Project of the National Natural Science Foundation of China (51705078) and the Fundamental Research Foundation of Sun Yat-sen University in 2019 (19lgpy300).

## References

1. Adel NH (2013) ASME Code development roadmap for HDPE pipe in nuclear service, ASME STP-NU-057. ASME Standards Technology, LLC, New York
2. Lai HS, Kil SH, Yoon KB (2015) Effects of defect size on failure of butt fusion welded MDPE pipe under tension. J Mech Sci Technol 29(5):1973–1980
3. Li H, Gao B, Dong J, Fu Y (2016) Welding effect on crack growth behavior and lifetime assessment of PE pipes. Polym Test 52:24–32
4. Kalyanam S, Krishnaswamy P, Shim DJ, Hioe Y, Focht E (2012) Structural integrity of HDPE piping and joints in nuclear safety-related applications. Proc 20th Int Conf Nucl Eng Asme 2012 Power Conf 4:51–62
5. Lai HS, Tun NN, Yoon KB, Hee SK (2016) Effects of defects on failure of butt fusion welded polyethylene pipe. Int J Press Vessel Pip 139-140:117–122
6. Farid VT, Mohammad RA (2017) Using developed creep constitutive model for optimum design of HDPE pipes. Polym Test 63: 392–397
7. Troughton M, Khamsehnezhad A (2016)Short-term and long-term mechanical testing to evaluate the effect of flaws in butt fusion joints in polyethylene pipes. Proceedings of the ASME Pressure Vessels and Piping Conference, Vancouver
8. Troughton M, Scandurra A (2002) Predicting the long-term integrity of butt fusion joints in polyethylene pipes. 17th International Plastic Fuel Gas Pipe Symposium, San Francisco
9. Li X, Bhushan B (2002) A review of nanoindentation continuous stiffness measurement technique and its applications. Mater Charact 48(1):11–36
10. Suwanprateeb J (2004) Rapid examination of annealing conditions for HDPE using indentation microhardness test. Polym Test 23(2): 157–161
11. Oliveira GL, Costa CA, Teixeira SCS, Costa MF (2014) The use of nano-and micro-instrumented indentation tests to evaluate viscoelastic behavior of poly (vinylidene fluoride) (PVDF). Polym Test 34:10–16
12. Lach R, Hutar P, Vesely P, Nezbedova E, Grellmann W (2013) Assessment with indentation techniques of the local mechanical behavior of joints in polymer parts. Polimery Warsaw 58(11): 900–905
13. Shaheer M, Troughton M, Khamsehnezhad A, Song J (2017) A study of the micro-mechanical properties of butt fusion-welded joints in HDPE pipes using the nanoindentation technique. Weld World 61(4):819–831
14. Huang CC, Wei MK, Lee S (2011) Transient and steady-state nanoindentation creep of polymeric materials. Int J Plast 27:1093–1102
15. Gao CH, Liu M (2017)Power-law creep of polycarbonate by Berkovich nanoindentation. Mater Res Express 4:105302
16. Adewole JK, Al-Mubaiyedh UA, Ul-Hamid A, Al-Juhani AA, Hussein IA (2012) Bulk and surface mechanical properties of clay modified HDPE used in liner applications. Can J Chem Eng 90(4): 1066–1078
17. Sahu SK, Badgayan ND, Samanta S, Sreekanth R (2018) Quasistatic and dynamic nanomechanical properties of HDPE reinforced with 0/1/2 dimensional carbon nanofillers based hybrid nanocomposite using nanoindentation. Mater Chem Phys 203: 173–184
18. Goodall R, Clyne TW (2006) A critical appraisal of the extraction of creep parameters from nanoindentation data obtained at room temperature. Acta Mater 54(20):5489–5499
19. Lucas BN, Oliver WC (1999) Indentation power-law creep of high-purity indium. Metall Mater Trans A - Physical Metall Mater Sci 30(3):601–610
20. Mayo MJ, Nix WD (1988) A micro-indentation study of super plasticity in Pb, Sn, and Sn-38 wt% Pb. Acta Metall 36(8):2183–2192
21. Veselý P, Kotter I, Lach R, Nezbedová E, Knésl Z, Hutař P, Grellmann W (2009) Prüfmethoden zur Analyse des lokalen mechanischen Verhaltens von Schweißnähten in Polyethylen-Kunststoffrohren, in: Borsutzki M, Geisler S (Eds.), Fortschritte der Kennwertermittlung für Forschung und Praxis, Proceedings Werkstoffprüfung 2009, 03./04.12.2009, Bad NeuenahrVerlag Stahleisen, Düsseldorf, 371-376.
22. Mikula J, Hutař P, Nezbedová E, Lach R, Arbeiter F, Ševčík M, Pinter G, Grellmann W, Náhlík L (2015) On crack propagation in the welded polyolefin pipes with and without the presence of weld beads. Mater Des 87:95–104
23. Lu S (2015) Formation of eigen-line in cold welding ultrasonic image of welded joints of polyethylene pipes. Zhejiang University, Zhejiang
24. Zeng XR, Gong KC, Gan WH, Weng KN (1999) Microhardness and DSC studies of HDPE compressed by ultrahigh pressure. Polym Mater Sci 15(3):113–115
25. Hyde TH, Saber M, Sun W (2010) Testing and modelling of creep crack growth in compact tension specimens from a P91 weld at 650 °C. Eng Fract Mech 77:2946–2957
26. Abson DJ, Rothwell JS (2013) Review of type IV cracking of weldments in 9-12%Cr creep strength enhanced ferritic steels. Int Mater Rev 58(8):437–473
27. Kimura K, Sawada K, Kushima H (2012) Creep rupture ductility of creep strength enhanced ferritic steels. J Press Vessel Technol 134: 031403-1-7